Dalton Transactions

RSC Publishing

PAPER

View Article Online
View Journal | View Issue

Cite this: *Dalton Trans.*, 2013, **42**, 3623

Decisive interactions that determine ferro/antiferromagnetic coupling in {3d–4f} pairs: a case study on dinuclear {V(IV)–Gd(III)} complexes†

Saurabh Kumar Singh and Gopalan Rajaraman*

Received 2nd October 2012,
Accepted 5th December 2012

DOI: 10.1039/c2dt32316h

www.rsc.org/dalton

The emerging class of mixed transition metal and lanthanide {3d–4f} complexes have gained more interest in recent years in the field of molecular magnetism. The key to success in this class of compounds lies in the nature of their observed magnetic coupling, which is mostly ferromagnetic. However several exceptions have emerged in recent years which makes understanding the origin of magnetic coupling crucial. DFT and CASSCF calculations have been performed on a structurally similar pair of {V(IV)–Gd(III)} complexes to underpin the dilemma of ferro/antiferromagnetic exchange interaction. We have chosen two structurally similar complexes, $[L^1V(O)Gd(H_2O)(NO_3)_3]$ (**1**); which displays a ferromagnetic interaction (J = +1.5 cm^{-1}) between the {V(IV)–Gd(III)} pair, while complex $[L^2V(O)\{(CH_3)_2CO\}Gd(NO_3)_3]$, (**2**) (see text for descriptions of L^1 and L^2) exhibits an antiferromagnetic exchange (J = −2.6 cm^{-1}). The DFT calculations yield J values of +2.0 cm^{-1} and −0.7 cm^{-1} for complexes **1** and **2** respectively and these values are in good agreement with the experimental values. CASSCF calculations have also been performed to understand the nature of the interaction in these complexes. The MO and NBO analysis demonstrate the importance of Gd(III) vacant 5d orbitals which contribute to the ferromagnetic part of the J values in this class of complexes. The extensive magneto-structural correlations developed suggests that a combination of two parameters, the V–O–Gd angle and the V–O–Gd–O dihedral angle, control the sign as well the magnitude of the J values. We have extended our studies to a tetranuclear $[L^3V(O)Gd(hfac)_2(CH_3OH)_2]_2$ complex to validate the proposed mechanism and the developed correlation. Our calculations also reveal that weak interactions are playing an important role in predicting the ground state for large polynuclear complexes.

Introduction

Single-Molecule Magnets (SMMs) have become an attractive prospect in the last decade due to a number of potential applications proposed.[1] Ideal SMMs possess a very large spin ground state and a sizable anisotropy – the combination which gives raise to a magnetization blockade at lower temperatures.[1,2] Numerous polynuclear clusters containing lanthanides have been reported with attractive blocking temperatures.[3] One recent example includes a $\{Dy(III)_5\}$ cluster reported to have a barrier height of 530 K –the largest reported for any cluster compound.[4] Despite these recent breakthroughs, the isolation of 4f-based SMMs with large barrier heights is challenging due to fast quantum tunnelling of magnetization and a weak exchange interaction.[2–4] These shortcomings can be overwhelmed, if mixed clusters of lanthanides and transition metal ions are targeted.[5] This is supported by the fact that, in the last decade, there are several novel {3d–4f} clusters reported with attractive blocking temperatures.[5–8]

Furthermore, the {3d–Gd} complexes are also attractive for other prospects such as magnetic refrigerants –one of the most promising applications for molecules built from paramagnetic metal ions.[9–11]

Key to the success of the {3d–4f} class of compounds lies in the nature of the magnetic interaction which is often found to be ferromagnetic, leading to the stabilization of a large spin ground state. There are some exceptions where the interaction is also found to be antiferromagnetic.[12,13] Despite several decades of synthetic efforts on {3d–4f} systems, the reason behind this anomaly is not fully understood.[14,15] One of the primary challenges in applying theoretical methods to this

Department of Chemistry, Indian Institute of Technology Bombay, Mumbai, India. E-mail: rajaraman@chem.iitb.ac.in; Fax: +91 022-25767152; Tel: +91 022-25767183

†Electronic supplementary information (ESI) available: DFT and CASSCF computed energies, for complex **1** and **2**, and DFT computed energies for complex **3**, computed overlap integrals, and spin densities of important atoms, simulation of the susceptibility behaviour for complex **3**, and CASSCF computed splitting of the f orbital. See DOI: 10.1039/c2dt32316h

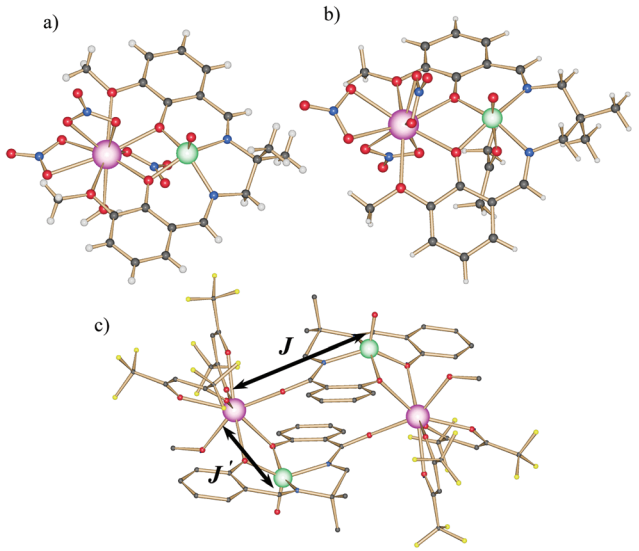

Fig. 1 Crystal structures of complexes (a) **1**, (b) **2** and (c) **3**. Gd(III) is in pink, V in light green, O in red, N in blue, H in white, F in yellow and C in black.

class of compounds is the inert nature of the 4f-orbitals which leads to the handling of the DFT broken symmetry scheme and also the electronic structure calculations are a delicate problem, as they often demand high level *ab initio* calculations to precisely address the problem of interest.[14,15] However our recent efforts with the DFT method combined with MO and NBO analysis were proven to be successful in computing the exchange and also in understanding the coupling mechanism in this class of compounds.[16] A pair of structurally similar compounds exhibiting ferro- and antiferromagnetic interaction respectively is required to probe the dilemma of intrinsic ferro-/antiferromagnetic interactions and also to examine the decisive interactions which determine the sign of coupling in this class of compounds.

Two dinuclear {VGd} complexes reported by Costes *et al.*[12] ($[L^1V(O)Gd(H_2O)(NO_3)_3]$, (**1**) where ($L^1$ = [*N*,*N*′-bis(3-methoxysalicylidene)-1,2-diamino-2-methylpropane]) and $[L^2V(O)\{(CH_3)_2CO\}Gd(NO_3)_3]$, (**2**) where ($L^2$ = [*N*,*N*′-bis(3-methoxysalicylidene)-1,3-diamino-2-2′-dimethyl-propane] see Fig. 1)) satisfy the primary requirement of structural resemblance. The magnetic studies reveal that compound **1** is ferromagnetic while **2** is antiferromagnetic, thus also satisfying the diverse property requirement. Therefore here we have chosen these two compounds as prototypes to understand the mechanism of coupling.

Here we have performed DFT and *ab initio* CASSCF studies on these compounds with the objective of (i) computing the magnetic exchange interaction *J*, (ii) comprehending the mechanism of coupling and (iii) developing reliable magneto-structural correlations for this pair. The study has also been extended to a tetrameric $\{V_2Gd_2\}$ complex ($[L^3V(O)Gd(hfac)_2(CH_3OH)_2]_2$, (**3**) where ($L^3$ = 2-hydroxy-*N*-{[(2-hydroxyphenyl)-methylene]amino}-2-methylpropyl) benzamide)[17] to cross-check the properties computed at the dimeric level.

Computational details

In the dinuclear complexes studied here, the magnetic exchange interaction between the V(IV) and Gd(III) ions is described by the following spin Hamiltonian,

$$\hat{H} = -J \cdot S_{Gd} \cdot S_V$$

where *J* is the isotropic exchange coupling constant and S_{Gd} and S_V are the spins on Gd(III) (S = 7/2) and V(IV) (S = 1/2) atoms respectively. DFT calculations combined with the Broken Symmetry (BS) approach[18] has been employed to compute the *J* values.

The BS method has a proven record of yielding good numerical estimates of *J* constants for a variety of complexes.[19–22] A detailed technical discussion on computational details on the evaluation of *J* values using the broken symmetry approach on dinuclear as well as trinuclear complexes can be found elsewhere.[21,22] Here, we have performed most of our calculations using the Gaussian 09 suite of programs.[23] We have employed a hybrid B3LYP functional[24] along with a double-zeta quality basis set employing the Cundari–Stevens (CS) relativistic effective core potential on Gd[25] and the TZV basis set on V[26] and the rest of the atoms (*level I*). A comprehensive method assessment performed earlier on {Cu–Gd} complexes by us, reveals that this combination yields good estimates of the *J* constants. We have also performed all electron calculations for comparison using the ORCA suite of programs[27] employing the SARC all electron basis set on Gd,[28] Ahlrichs and co-workers TZVP on V[26] along with their SVP basis set on the rest of the elements. These calculations have been performed by incorporating relativistic effects *via* the Douglas–Kroll–Hess method[29] (*level II*). A very tight SCF convergence has been employed throughout. All magneto-structural calculations have been performed by varying the specific structural parameters and performing single point calculations on the modified structure.

For tetranuclear complexes the following spin Hamiltonian has been adopted,

$$\hat{H} = -J \cdot S_{Gd_1} \cdot S_{V_1} - J' \cdot S_{Gd_1} \cdot S_{V_2}$$

The magnetic exchange interactions in tetranuclear complexes were extracted using a pair-wise interaction model[19] where four spin configurations are computed to extract three different exchange interactions (J_1–J_3). The following five spin configurations have been computed: (i) all spin up (S = 8), (ii) spin down on only V_2 (S = 7), (iii) spin down on only Gd_1 (S = 1), (iv) spin down on both V_1 and V_2 (S = 6), (v) spin down on Gd_2 and V_2 (S = 0). The energy differences between the spin configurations are equated to the corresponding exchange interactions from which the two *J* values have been extracted.

In the *ab initio* framework, all calculations have been performed using complete active space self-consistent theory (CASSCF) as implemented in the ORCA software with the SARC basis set for Gd(III), TZV for V(IV) and SVP for the remaining

atoms. The calculations have been performed with the SV/C correlation fitting basis sets. The SCF calculations are tightly converged (1×10^{-8} E_h in energy). We have taken eight electrons ($f^7 + d^1$) with 12 active orbitals (8, 12) as a reference space.

Result and discussion

In both complexes **1** and **2** the metal ions are doubly bridged by two μ-phenolato bridges (Fig. 1). However there are some minute structural differences, for example in **1** the {GdO_2V} core is almost planar while in complex **2** it is twisted with a V–O–Gd–O dihedral angle of 18.0°. The Gd(III) is deca-coordinated in both complexes with Gd···V separations of 3.519 Å and 3.504 Å in **1** and **2**, respectively. The geometry around V(IV) also differs with a penta-coordination in **1** and a hexa-coordination in complex **2**. The average V–O–Gd bond angles are 107.1° and 105.4° for complexes **1** and **2** respectively. Complex **3** is a tetranuclear complex with two heterodinuclear [V(O)-L^3Gd(hfac)] units linked through two oxygen atoms of the L^3 ligand (see Fig. 1c). The V(IV) units are square-pyramidal with the Gd(III) exhibiting a coordination number of eight. The two {VGd} dimers are well separated by a Gd–O–C–N–V bridge with the V···V and Gd···Gd distance of 6.559 Å and 7.792 Å respectively. The V–O–Gd angles are found to be 106.4° and V–O–Gd–O dihedral angles are 15.1°. Studies performed on complexes **1** and **2** are discussed initially with the results from studies on complex **3** discussed in the subsequent section.

The experimental magnetic susceptibility studies carried out on a polycrystalline sample of **1** identify a ferromagnetic exchange between the V(IV) and Gd(III) ions with a J value of +1.5 cm^{-1}, while an antiferromagnetic exchange is observed in **2** with a J value of −2.6 cm^{-1}. Our DFT calculated value for **1** is +2.2 cm^{-1} while for **2** it is −0.7 cm^{-1}. The sign of these J values were reproduced by our calculations, albeit the magnitude slightly deviates from the experimental value in both cases (the computed total energies together with $<S^2>$ expectation values of complexes and their models are listed in Tables S1–S3 of ESI†). The computed spin density plot together with the magnetic orbitals of V(IV) in complex **1** is shown in Fig. 2. The spin densities on V(IV) (1.15) and Gd(III) (7.02) ions are found to be *ca.* the same in both the complexes, suggesting a spin polarisation mechanism by which both the ions gain spin densities (see ESI Table S4 and Fig. S1† for labels and values).

A schematic mechanism of coupling developed in earlier years invoking a charge transfer path where a partial charge transfer from the 3d orbitals of the metal ion to the empty 5d/6s orbitals of the Gd(III) atom was proposed.[30,31] A more quantitative mechanism for the {3d–4f} pair emerges from an *ab initio* CASSCF/PT2 study[14] and a series of DFT calculations.[15,16,32] The following concise points emerge with respect to the mechanism of coupling for a generic {3d–4f} pair: (i) the net J value has contributions from both J_F (the ferromagnetic part of J) and J_{AF} (the antiferromagnetic part of J)

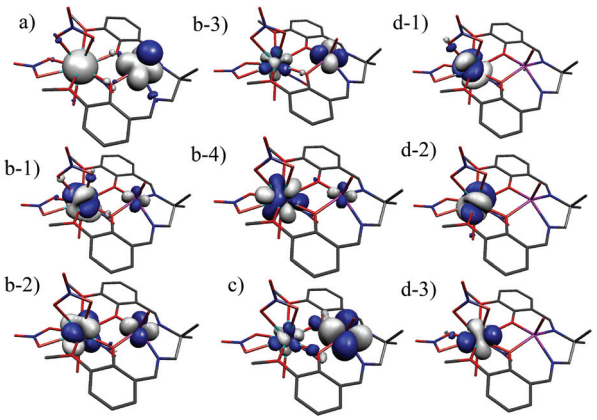

Fig. 2 The CASSCF magnetic orbital of V(IV) and Gd(III) (a) spin density plot of **1**, (b-1) to (b-4) four sets of non-orthogonal orbitals, (c) d_{xy} orbital of V(IV), (d-1) to (d-3) three sets of orthogonal orbital of Gd(III). All the orbitals plotted are for the $S = 9/2$ high spin state. The isodensity surface represented corresponds to a value of 0.03 e^- $bohr^{-3}$.

parts and the sign of the exchange is decided by the dominating factor; (ii) the J_F arise due to two contributions (a) orthogonality between 3d- and 4f-magnetic orbitals and (b) charge transfer to empty 5d orbitals of the 4f-ions; (iii) the J_{AF} has contributions due to the non-orthogonality between the 3d- and the 4f-magnetic orbitals.

MO and NBO analysis can offer clues to the J_F and J_{AF} contributions to the net exchange. The unpaired electron in V(IV) is found to reside in the d_{xy} orbital and the overlap integral computed between the d_{xy} and the seven f-orbitals of the Gd(III) ion reveals that there are several significant overlap values detected for complex **2** when compared to complex **1** (see Table S5, ESI† for computed overlap values). This primarily suggests that complex **2** has larger J_{AF} contributions. To obtain further clues into the orthogonality/non-orthogonality of the magnetic orbitals, *ab initio* CASSCF calculations have been performed on complexes **1** and **2** (see computational details). The CASSCF computed J values are found to be +1.08 cm^{-1} for **1** and +0.6 cm^{-1} for **2**. The CASSCF calculations did not reproduce the sign of exchange in complex **2** however the trend of **1** being more ferromagnetic than **2** is correctly reproduced. The reproduction of the sign in this method might require a larger reference space including empty 5d/6s orbitals of Gd(III).[14]

The CASSCF orbitals of complex **1** are shown in Fig. 2. Interestingly, the CASSCF orbitals fall into two distinct classes, four 4f-orbitals are found to be orthogonal as they do not mix with the V(d_{xy}) orbital and three are found to be non-orthogonal, where significant 4f–d_{xy} mixing is apparent.

These two sets eventually contribute to J_F and J_{AF} respectively. Most importantly the f_{xyz} orbital of the 4f ion is found to interact with the d_{xy} orbital of the V(IV) metal centre. The extent of mixing as revealed in the computed MO coefficients suggests that in **1** it is about 16% while in **2** it is about 27% (see Fig. 3). This particular orbital is found to be relatively higher in energy compared to other f-orbitals and the f-orbital

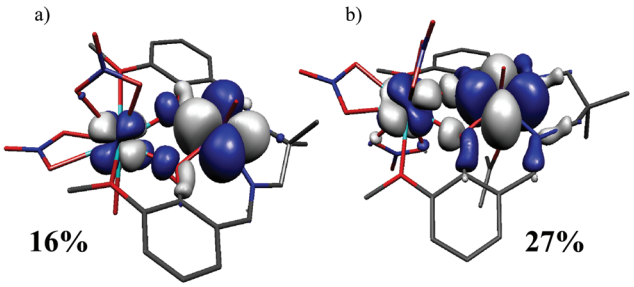

Fig. 3 The plot of the $4f_{xyz}$–$3d_{xy}$ interaction for complex (a) **1** and (b) **2** showing % contribution from the 4f-orbital in each case. The isodensity surface represented corresponds to a value of 0.03 e^{-} $bohr^{-3}$. The grey and blue region indicates the positive and negative densities. The plotted orbitals are for $S = 7/2$ low spin state.

splitting in **2** is found to be larger than that of complex **1** (see Fig. S2†). This interaction is found to be decisive in deciding the nature of coupling for this pair. Moreover the overlap integral obtained from the DFT calculations also supports these numbers (see Table S5†). The NBO analysis reveals that the 5d occupation found on the Gd(III) atoms in both complexes also differ slightly revealing a larger J_F contribution to **1**. Thus a larger J_{AF} and a smaller J_F contribution led to a switch from ferromagnetic to antiferromagnetic interactions in **2**. Now the question is why?

Magneto-structural correlations

Checks were made on the ligand environment particularly the coordination number of V(IV). The coordination environment (square pyramidal *vs.* octahedral) is found to differ between **1** and **2** but has negligible effect on coupling (square pyramidal model of **2** yields a J value of -0.62 cm^{-1} (see Fig. S3, ESI†)). Apart from the number of bridges, the structural parameters that are likely to affect the magnetic coupling are the V–O and Gd–O bond distances, the V–O–Gd bond angle, the V–O–Gd–O dihedral angle and the out-of-plane shift of the bridging phenoxo group, τ.[33] To answer the specific question as to which parameter controls the nature of the magnetic interaction, we have developed magneto-structural correlations for these parameters (see Fig. 4). The average V–O and Gd–O distances between **1** and **2** are 2.16 Å and 2.19 Å while the bond angle is 107.5° in **1** and 105° in **2**. A large variance is detected in the dihedral angle (3.2° for **1** *vs.* 18° for **2**) and the τ parameter (8.3° for **1** *vs.* 25.2° for **2**).

Bond distance. As shown in Fig. 4a, when the average bond distance was increased from 2.2 Å, the J value decreases initially and then it tends to become more static at larger bond distances, however the correlation stays within the ferromagnetic regime. As the V–O; Gd–O bond elongates, it effectively reduces the charge transfer path from V(3d) → Gd(5d) and this results in a decrease in ferromagnetic coupling. However comparison to the experimental parameters suggests a large deviation from the experimental values for other structures and thus this parameter is unlikely to control the sign of the magnetic exchange.

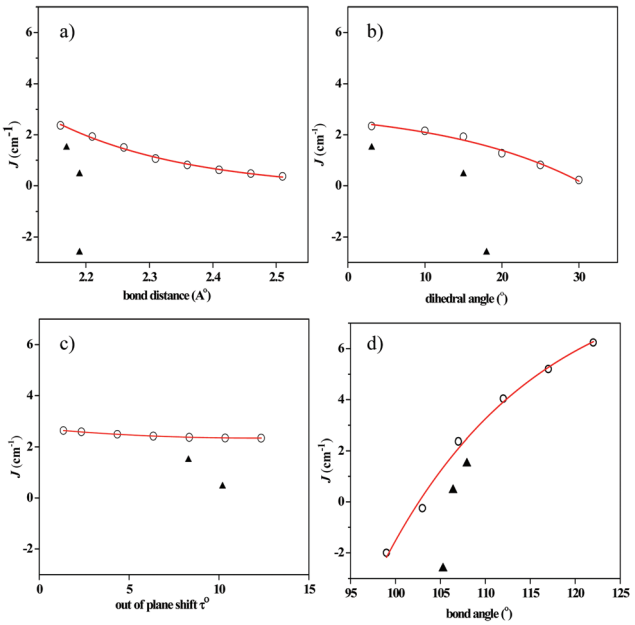

Fig. 4 Magneto-structural correlations developed by varying different structural parameters for complex **1** (a) average V–O; Gd–O bond distances (in Å), (b) V–O–Gd–O dihedral angle, (c) out of plane shift τ, (d) average V–O–Gd bond angles. Here, open circles are DFT computed points while the red line represent the best fit to these points. Solid triangles represent points from experimental structures with the corresponding J values.

Dihedral angle. A second correlation is developed by varying the V–O–Gd–O torsional angle (Fig. 4b). From the figure it is clear that the planar structure with zero torsional angle has the largest ferromagnetic exchange. Larger torsional angles lead to lower J values, similar to that found for the other {3d–Gd} pairs.[16] The experimental points are rather scattered here, presumably suggesting that the dihedral angle might not be the exclusive structural parameter which controls the magnetic exchange.

Out-of-plane-shift (τ). The out-of-plane-shift τ describes the deviation of the phenyl ring from the V–O–Gd–O plane. This parameter has been previously shown to be important in accounting for the differences in J values across structures in transition metal and {3d–4f} complexes.[34] Here an exponential relationship has been detected with larger τ leading to smaller J values. However, looking at the y-axis it is straightforward to conclude that the variation in J is negligible and thus τ is unlikely to control the sign or the magnitude of the J value in this pair.

Bond angle. The correlation developed when varying the V–O–Gd angle is shown in Fig. 4d. An exponential relationship to J has been observed, and more importantly a switch from ferro- to antiferromagnetic exchange has been detected at 103.4°. As the angle increases, the J_F contribution increases leading to smaller J values for the antiferromagnetic regime and larger J values for the ferromagnetic regime (see Table S6 and Fig. S4, ESI†). Moreover, we have plotted the computed Gd(III) 5d and 6s orbital occupation number *vs.* bond angle (see Fig. 5a) and this gives an important insight into the

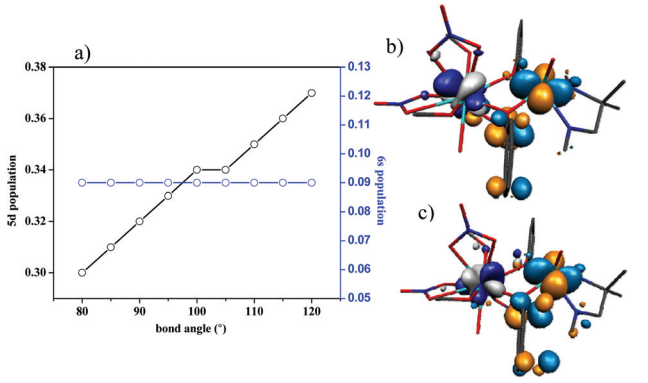

Fig. 5 (a) NBO computed 5d and 6s population with variation of the V–O–Gd bond angle. Superimposed BS-DFT orbital of f_{xyz} and d_{xy} for bond angle (b) 99.0° and (c) 103.5 degrees. The isodensity surface represented corresponds to a value of 0.03 e^- $bohr^{-3}$.

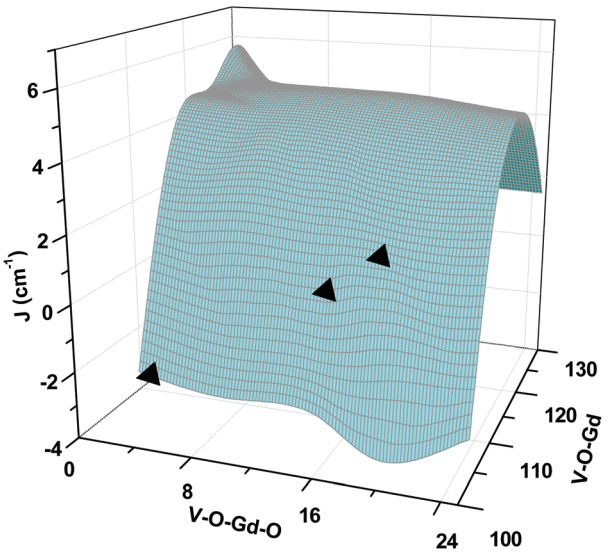

Fig. 6 The magneto-structural correlation developed for complex **1** by varying V–O–Gd angle and V–O–Gd–O dihedral angle (°) simultaneously. The black triangle represent the experimental points.

mechanism of coupling. As evident from the figure, the 5d occupation increases linearly as the angle increases, suggesting that the J_F contribution increases. On the other hand, the occupation number of the 6s orbital of the Gd(III) ion remains constant. This strongly supports the earlier proposed mechanism of coupling.[16] Mapping the available experimental points to the computed curves suggests that this bond angle might be a suitable parameter to describe the magnetic coupling in this {V(IV)–Gd(III)} pair. In addition, the variation in J observed with other parameters are minimal compared to this particular bond angle. A similar conclusion has also been previously drawn for the {Ni(II)–Gd(III)} pair.[16]

Since a switch from ferro- to antiferromagnetic exchange is observed with this correlation, we have attempted to cross-check our decisive interaction d_{xy}–f_{xyz}. As we have previously stated, as the angle decreases from 105.5° to 99.0°, the overlap integral for the d_{xy}–f_{xyz} pair should increase significantly. Our overlap calculations support this statement (see Table S6† and Fig. 5b and 5c for the corresponding orbital plots) and thus provide confidence to the determined decisive interaction.

Hybrid correlation. An exponential relationship of the J value to the bond angle has been found; however fitting the points to an exponential relationship (see ESI† for details) does not predict an antiferromagnetic switch at an angle of 105° as observed in complex **2**. Furthermore a large variation in the dihedral angle between **1** and **2** demands its inclusion in the magneto-structural correlation. To explore if more than one parameter can offer a rational for the switch, we have developed a three dimensional magneto-structural correlation by varying both the bond angles and the dihedral angles simultaneously (Fig. 6). This correlation is able to reproduce the sign at 105° of the V–O–Gd bond angle and at 18° of V–O–Gd–O dihedral angle.[35] The developed correlation has severe depth and crest, suggesting interplay of both the parameters in deciding the sign and the magnitude of the exchange. It is very clear from this analysis that more than one parameter might be required to rationalise the magnetic exchange and one has to bear this in mind while interpreting/rationalizing the experimental data.

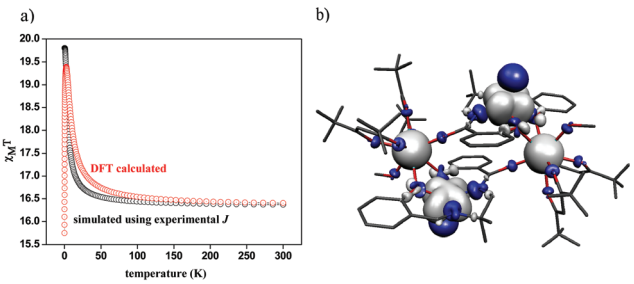

Fig. 7 (a) Thermal variation of $\chi_M T$ for complex **3** up to 0.2 K. The black curve represents simulation using experimental J values (J_{V-Gd} = +0.46 cm^{-1} and J' = 0), while the red curve represents simulation with DFT values. See ref. 17 for the experimental data. (b) DFT computed spin density plot for complex **3**, the white and blue region indicates positive and negative spin densities. The isodensity surface represented corresponds to a value of 0.03 e^- $bohr^{-3}$.

Studies on the tetranuclear {V_2(IV)–Gd_2(III)} complex

To analyse the precise conclusions derived from the mechanism of coupling and the magneto-structural correlations for the {V(IV)–Gd(III)} pair, we have extended our study to a tetrameric {V_2(IV)–Gd_2(III)} complex, complex **3**, (see Fig. 1).[17] The experimental magnetic susceptibility of **3** is fit by assuming there is no interaction between the dimers (J') while within the {VO_2Gd} dimeric unit the fit yields the J_{V-Gd} value of +0.46 cm^{-1} (see Fig. 7a). This results in an S = 4 ground state for **3**, which was also confirmed from magnetization data. Our DFT calculations give a J_{V-Gd} value of +0.94 cm^{-1}. The sign as well the magnitude is reproduced reasonably well with the

DFT.[16] Furthermore the magnitude can be rationalised by taking into consideration the V–O–Gd angle and the V–O–Gd–O dihedral angles, which were found to be between those observed for complexes **1** and **2**. This adds confidence to the developed magneto-structural correlation.

More importantly, we have also computed the exchange interaction between the dimeric (J') units and in contrast to the experiment, this is found to be antiferromagnetic in nature with a value of -0.01 cm^{-1}. It should be noted that although the computed J value is small, the actual energy difference between different spin configurations are *ca.* 0.1 cm^{-1}. Although this gap is too large to be trusted as reported earlier,[36] one has to be cautious as the values are at the limit of the employed theoretical methods. This weak antiferromagnetic exchange drastically affects the conclusions, *i.e.* with a weak antiferromagnetic exchange between the {VO_2Gd} units, the ground state is calculated to be $S = 0$ in contrast to $S = 4$ as suggested by the experiment. Our calculated J values provide a good fit to the experimental curve up to 1.2 K, below which the $\chi_M T$ value decreases drastically (see Fig. 7a and Fig. S4, ESI†). Since the experiment is performed only up to 2 K, this downturn has not been observed. This invariably suggests that to precisely elucidate the ground state of such complexes, one might need to reach lower temperatures. The spin density plot computed for **3** is shown in Fig. 7b. The significant amount of spin densities observed on the spacer atoms suggests that the J' interaction is unlikely to be zero as assumed in the experiments (see Fig. S5, ESI†). It should be noted here that a dimer-of-dimers structural topology with a weak inter-dimer interaction has been reported in several instances to have potential applications in quantum computing.[37]

Conclusions

For the first time combined DFT and CASSCF calculations have been employed to compute the magnetic exchange parameters (J) and comprehend the mechanism of coupling in ferro-/antiferromagnetically coupled dinuclear {VGd} complexes. DFT correctly predicts the sign of their associated J values and CASSCF orbitals offer a significant insight into the mechanism of coupling, where a decisive f_{xyz}–d_{xy} interaction has been detected and found to be imperative in determining the sign of the exchange. Our NBO analysis indicates that the empty 5d orbital of Gd(III) contributes to the ferromagnetic part of the exchange similar to that found in other {3d–Gd} pairs. Our magneto-structural studies reveal that it is not always one unique parameter that is important in determining the J value, here the V–O–Gd bond angles and V–O–Gd–O dihedral angles combination was found to play an active role in switching the exchange from ferro- to antiferromagnetic. Our studies on the tetramer {V_2(IV)–Gd_2(III)} offers some significant insight into the magnetic properties of this complex. A weak antiferromagnetic J' value suggests an $S = 0$ ground state for this molecule. When taking into account the strength of the J value observed here, low temperature measurements might be required to unequivocally determine the ground state for such clusters.

Acknowledgements

GR would like to acknowledge financial support from the Government of India through the Department of Science and Technology (SR/S1/IC-41/2010) and the Indian Institute of Technology, Bombay to access the high performance computing facility. SKS would like to thanks IIT-Bombay for SRF fellowship.

Notes and references

1 (*a*) R. Sessoli, D. Gatteschi, A. Caneschi and M. A. Novak, *Nature*, 1993, **365**, 141; (*b*) G. Christou, D. Gatteschi, D. N. Hendrickson and R. Sessoli, *Mater. Res. Bull.*, 2000, **25**, 66; (*c*) D. Gatteschi, R. Sessoli and J. Villain, *Molecular Nanomagnets*, Oxford University Press, Oxford, 2006.

2 A. Caneschi, D. Gatteschi and R. Sessoli, *Angew. Chem., Int. Ed.*, 2003, **42**, 268.

3 (*a*) P.-H. Lin, T. J. Burchell, L. Ungur, L. F. Chibotaru, W. Wernsdorfer and M. Murugesu, *Angew. Chem., Int. Ed.*, 2009, **48**, 9489; (*b*) B. Hussain, D. Savard, T. J. Burchell, W. Wernsdorfer and M. Murugesu, *Chem. Commun.*, 2009, 1100.

4 R. J. Blagg, C. A. Muryn, E. J. L. McInnes, F. Tuna and R. E. P. Winpenny, *Angew. Chem., Int. Ed.*, 2011, **50**, 6530.

5 R. Sessoli and A. Powell, *Coord. Chem. Rev.*, 2009, **253**, 2328.

6 (*a*) C. Zaleksi, E. Depperman, J. Kamf, M. Kirk and V. Pecoraro, *Angew. Chem., Int. Ed.*, 2004, **43**, 3912; (*b*) J. Rinck, G. Novitchi, W. Van Den Heuvel, L. Ungur, Y. Lan, W. Wernsdorfer, C. E. Anson, L. F. Chibotaru and A. K. Powell, *Angew. Chem., Int. Ed.*, 2010, **49**, 7583; (*c*) J.-P. Costes, F. Dahan and J. Garcia-Tojal, *Chem.–Eur. J.*, 2002, **8**, 5430; (*d*) J.-P. Costes, F. Dahan, A. Dupuis and J. P. Laurent, *Inorg. Chem.*, 1997, **36**, 4284.

7 (*a*) N. F. Chilton, S. K. Langley, B. Moubaraki and K. S. Murray, *Chem. Commun.*, 2010, **46**, 7787; (*b*) S. K. Langley, L. Ungur, N. F. Chilton, B. Moubaraki, L. F. Chibotaru and K. S. Murray, *Chem.–Eur. J.*, 2011, **17**, 9209; (*c*) S. Igarashi, S.-I. Kawaguchi, Y. Yukawa, F. Tuna and R. E. P. Winpenny, *Dalton Trans.*, 2009, 3140.

8 (*a*) J. Rinck, G. Novitchi, W. V. Heuvel, L. Ungur, Y. Lan, W. Wernsdorfer, C. E. Anson, L. F. Chibotaru and A. K. Powell, *Angew. Chem., Int. Ed.*, 2010, **49**, 7583; (*b*) H. L. C. Feltham, R. Clerac, A. K. Powell and S. Brooker, *Inorg. Chem.*, 2011, **50**, 4232.

9 (*a*) G. Karotsis, S. Kennedy, S. J. Teat, C. M. Beavers, D. A. Fowler, J. J. Morales, M. Evangelisti, S. J. Dalgarno and E. K. Brechin, *J. Am. Chem. Soc.*, 2010, **132**, 12983; (*b*) T. N. Hooper, J. Schnack, S. Piligkos, M. Evangelisti and

E. K. Brechin, *Angew. Chem., Int. Ed.*, 2012, **51**, 4633; (*c*) T. Birk, K. S. Pedersen, C. Thuesen, T. Weyhermüller, M. Schau-Magnussen, S. Piligkos, H. Weihe, S. Mossin, M. Evangelisti and J. Bendix, *Inorg. Chem.*, 2012, **51**, 5435.

10 (*a*) Y.-Z. Zheng, E. M. Pineda, M. Helliwell and R. E. P. Winpenny, *Chem.–Eur. J.*, 2012, **18**, 4161; (*b*) M. Evangelisti and E. K. Brechin, *Dalton Trans.*, 2010, **39**, 4672; (*c*) Y.-Z. Zheng, M. Evangelisti and R. E. P. Winpenny, *Angew. Chem., Int. Ed.*, 2011, **50**, 3692.

11 S. K. Langley, N. F. Chilton, B. Moubaraki, T. Hooper, E. K. Brechin, M. Evangelisti and K. S. Murray, *Chem. Sci.*, 2011, **2**, 1166.

12 J.-P. Costes, F. Dahan, B. Donnadieu, J. Garcia-Tojal and J.-P. Laurent, *Eur. J. Inorg. Chem.*, 2001, 363.

13 A. N. Gerogopolou, R. Adam, C. P. Raptopoulou, V. Psycharis, R. Ballesteros, B. Abarca and A. K. Boudalis, *Dalton Trans.*, 2010, 5020.

14 V. Paulovic, F. Cimpoesu, M. Ferbinteanu and K. Hirao, *J. Am. Chem. Soc.*, 2004, **126**, 3321.

15 (*a*) E. Cremades, S. Gómez-Coca, D. Aravena, S. Alvarez and E. Ruiz, *J. Am. Chem. Soc.*, 2012, **134**, 10532; (*b*) F. Cimpoesu, F. Dahan, S. Ladeira, M. Ferbinteanu and J.-P. Costes, *Inorg. Chem.*, 2012, **51**, 11279; (*c*) M. Ferbinteanu, F. Cimpoesu, M. A. Girtu, C. Enachescu and S. Tanase, *Inorg. Chem.*, 2012, **51**, 40.

16 (*a*) G. Rajaraman, F. Totti, A. Bencini, A. Caneschi, R. Sessoli and D. Gatteschi, *Dalton Trans.*, 2009, 3153; (*b*) S. K. Singh, N. K. Tiberewal and G. Rajaraman, *Dalton Trans.*, 2011, **40**, 10897; (*c*) T. Rajeshkumar and G. Rajaraman, *Chem. Commun.*, 2012, **48**, 7856; (*d*) T. Rajeshkumar, S. K. Singh and G. Rajaraman, *Polyhedron*, 2013, DOI: 10.1016/j.poly.2012.06.017; (*e*) N. Berg, T. Rajeshkumar, S. M. Taylor, E. K. Brechin, G. Rajaraman and L. F. Jones, *Chem.–Eur. J.*, 2012, **18**, 5906.

17 J.-P. Costes, S. Shova, J. Modesto, C. Juan and N. Suet, *Dalton Trans.*, 2005, 2830.

18 L. Noodleman, *J. Chem. Phys.*, 1981, **74**, 5737.

19 E. Ruiz, S. Alvarez, A. Rodriguez-Fortea, P. Alemany, Y. Pouillon and C. Massobrio, in *Magnetism: Molecules to Materials*, ed. J. S. Miller and M. Drillon, Wiley-VCH, Weinheim, 2001, vol. II, p. 227.

20 S. Piligkos, G. Rajaraman, M. Soler, N. Kirchner, J. van Slageren, R. Bircher, S. Parsons, H. Guedel, J. Kortus, W. Wernsdorfer, G. Christou and E. K. Brechin, *J. Am. Chem. Soc.*, 2005, **127**, 5572.

21 (*a*) E. Ruiz, S. Alvarez, J. Cano and P. Alemany, *J. Comput. Chem.*, 1999, **20**, 1391; (*b*) E. Ruiz, A. R. Fortea, J. Cano, S. Alvarez and P. Alemany, *J. Comput. Chem.*, 2003, **24**, 982; (*c*) E. Ruiz, J. Cano, S. Alvarez, A. Caneschi and D. Gatteschi, *J. Am. Chem. Soc.*, 2003, **152**, 6791; (*d*) G. Rajaraman, J. Cano, E. K. Brechin and E. J. L. McInnes, *Chem. Commun.*, 2004, 1476.

22 P. Christian, G. Rajaraman, A. Harrison, M. Helliwell, J. J. W. McDouall, J. Raftery and R. E. P. Winpenny, *Dalton Trans.*, 2004, 2550.

23 M. J. Frisch, G. W. Trucks, H. B. Schlegel, G. E. Scuseria, M. A. Robb, J. R. Cheeseman, G. Scalmani, V. Barone, B. Mennucci, G. A. Petersson, H. Nakatsuji, M. Caricato, X. Li, H. P. Hratchian, A. F. Izmaylov, J. Bloino, G. Zheng, J. L. Sonnenberg, M. Hada, M. Ehara, K. Toyota, R. Fukuda, J. Hasegawa, M. Ishida, T. Nakajima, Y. Honda, O. Kitao, H. Nakai, T. Vreven, J. A. Montgomery Jr., J. E. Peralta, F. Ogliaro, M. Bearpark, J. J. Heyd, E. Brothers, K. N. Kudin, V. N. Staroverov, R. Kobayashi, J. Normand, K. Raghavachari, A. Rendell, J. C. Burant, S. S. Iyengar, J. Tomasi, M. Cossi, N. Rega, J. M. Millam, M. Klene, J. E. Knox, J. B. Cross, V. Bakken, C. Adamo, J. Jaramillo, R. Gomperts, R. E. Stratmann, O. Yazyev, A. J. Austin, R. Cammi, C. Pomelli, J. W. Ochterski, R. L. Martin, K. Morokuma, V. G. Zakrzewski, G. A. Voth, P. Salvador, J. J. Dannenberg, S. Dapprich, A. D. Daniels, Ö. Farkas, J. B. Foresman, J. V. Ortiz, J. Cioslowski and D. J. Fox, *GAUSSIAN 09 (Revision A.1)*, Gaussian, Inc., Wallingford, CT, 2009.

24 A. D. Becke, *J. Chem. Phys.*, 1993, **98**, 5648.

25 T. R. Cundari and W. J. Stevens, *J. Chem. Phys.*, 1993, **98**, 5555.

26 A. Schafer, C. Huber and R. Ahlrichs, *J. Chem. Phys.*, 1994, **100**, 5829.

27 F. Neese, *Orca, 2.6.2360*, Bonn, 2010.

28 D. A. Pantazis and F. Neese, *J. Chem. Theor. Comput.*, 2009, **5**, 2229.

29 M. Douglas and N. M. Kroll, *Ann. Phys.*, 1974, **82**, 89.

30 (*a*) C. Benelli, A. Caneschi, D. Gatteschi, O. Guillou and L. Pardi, *Inorg. Chem.*, 1990, **29**, 1750; (*b*) C. Benelli, A. Caneschi, D. Gatteschi and R. Sessoli, *J. Appl. Phys.*, 1993, **73**, 5333.

31 (*a*) O. Kahn and O. Guillou, in *Research Frontiers in Magnetochemistry*, ed. C. J. O'Conner, World Scientific, Singapore, 1993, p. 179; (*b*) O. Kahn, *Angew. Chem., Int. Ed. Engl.*, 1985, **24**, 834; (*c*) O. Kahn, *Molecular Magnetism*, VCH Publishers, New York, 1993.

32 (*a*) J. Cirera and E. Ruiz, *C. R. Chim.*, 2008, **11**, 1227; (*b*) J. Kortus, M. R. Pederson, T. Baruah, N. Bernstein and C. S. Hellberg, *Polyhedron*, 2003, **22**, 1871.

33 (*a*) E. Ruiz, T. Cauchy, J. Cano, R. Costa, J. Tercero and S. Alvarez, *J. Am. Chem. Soc.*, 2008, **130**, 7420; (*b*) E. Ruiz, *Structure and Bonding*, Springer, Berlin, Germany, 2004, 113.

34 E. Ruiz, J. Cano, S. Alvarez and P. Alemany, *J. Am. Chem. Soc.*, 1998, **120**, 11122.

35 Since the sign and magnitude is reproduced with angle and dihedral, other simultaneous structural variations have not been attempted.

36 S. Gómez-Coca, E. Ruiz and J. Kortus, *Chem. Commun.*, 2009, 4363.

37 (*a*) M. Affronte, *J. Mater. Chem.*, 2009, **19**, 1731; (*b*) G. A. Timco, S. Carretta, F. Troiani, F. Tuna, R. G. Pritchard, E. J. L. McInnes, A. Ghirri, A. Candini, P. Santini, G. Amoretti, M. Affronte and R. E. P. Winpenny, *Nat. Nanotechnol.*, 2009, **4**, 173; (*c*) C.-F. Lee, D. A. Leigh,

R. G. Pritchard, D. Schultz, S. J. Teat, G. A. Timco and R. E. P. Winpenny, *Nature*, 2009, **458**, 314; (*d*) G. A. Timco, T. B. Faust, F. Tuna and R. E. P. Winpenny, *Chem. Soc. Rev.*, 2011, **40**, 3067; (*e*) G. Aromi, D. Aguila, P. Gamez, F. Luis and O. Roubeau, *Chem. Soc. Rev.*, 2012, **41**, 537; (*f*) F. L. Mettes, G. Aromi, F. Luis, M. Evangelisti, G. Christou, D. Hendrickson and L. J. de Jongh, *Polyhedron*, 2001, **20**, 1459; (*g*) S. Hill, R. S. Edwards, N. Aliaga-Alcalde and G. Christou, *Science*, 2003, **302**, 1015.

